6. ANKARA INTERNATIONAL AEROSPACE CONFERENCE AIAC-2011-036
14-16 September 2011 - METU, Ankara TURKEY

COMPUTATIONAL FLUID DYNAMICS ANALYSIS OF A DUCTED ROTOR

Yüksel Ortakaya[1], A. Alper Ezertaş[2] and Emre Yazıcı[3]
Turkish Aerospace Industries, Inc.
Ankara,Turkey

ABSTRACT

Numerical simulation of turbulent flow around a ducted rotor is performed and aerodynamic performance of this configuration is evaluated. The flow field is analyzed with a computational fluid dynamics (CFD) solver and k-ω SST turbulence model. The rotor is simulated with two different approaches; one is rotating reference frame and periodic boundary condition and the other is blade element-momentum method based boundary condition which is used as an alternative and fast solution strategy. To validate the flow solution approaches, results obtained from both approaches are compared with the results available in literature.

INTRODUCTION

Ducted tail rotor design is one of the most efficient antitorque generation systems for helicopters, since it supplies superior performance in terms of aerodynamics, noise and safety compared to its conventional counterparts. In the last two decades, with the intensive research on improving efficiency of tail rotors, most of the helicopter manufacturers have developed their own ducted tail rotor designs such as FENESTRON [1], FANTAIL [2] and FAN-IN-FIN [3]. The simulation of ducted tail rotor aerodynamics is still not a mature area [4, 5, 6, 7, 8, 9, 10, 11], and improvement in this field has potential in terms of building more efficient future rotorcraft.

Better understanding of the aerodynamics of ducted fan systems will lead to more effective designs. In this context, CFD is a vital tool to analyze, understand and improve the aerodynamics of ducted rotor systems. Today, it is possible to analyze flow field details of ducted rotors such as blade tip losses, end wall effects and separation of the flow at the duct lip. This analysis capability provides potential for innovative systems design. Various aerodynamic analyses efforts for ducted tail rotor configurations have been published in the last decade. Although the flow field is analyzed with Euler or Navier-Stokes flow solvers in these studies, rotor simulations show variations. Rajagopalan and Keys analyzed the Fantail type tail rotor with time averaged momentum source terms [4]. Boris and Serguei evaluated the Fan-in-Fin configuration by simulating the rotor using an ideal vortex theory [5]. Alpman and Long simulated the tail rotor by the actuator disk model [6]. Costes et al. analyzed the Fenestron with the actuator disk model [7]. Ruzicka and Strawn simulated the Fantail with the Discrete Blade Modeling [8]. Nygaar et. al. analyzed the same case with improved Momentum Source Model [9]. Kwon et al studied the shrouded tail rotor with periodic boundary condition [10] and compared the results with the experimental ones published by Boris et .al [5]. Cao et al. modeled a ducted tail rotor by time-averaged momentum source terms [11].

The aim of this study is to solve a validation problem for the ducted rotor configuration and evaluate the flow solver for future ducted rotor design and analysis needs. In this study, CFD analyses are performed to analyze the aerodynamic performance of the ducted tail rotor in hover. The utilized CFD analysis tool is a commercial Reynolds averaged Navier-Stokes solver with k- ω SST turbulence

[1] Chief of Aeromechanic Group, Integrated Helicopter Systems Email: yortakaya@tai.com.tr
[2] Design Engineer, Aeromechanic Group, Integrated Helicopter Systems Email: aezertas@tai.com.tr
[3] Executive Vice President, Integrated Helicopter Systems Email: eyazici@tai.com.tr

model. The main approach used to simulate the rotor can be summarized by defining a rotating reference frame for the flow domain around a single rotor blade and analyzing with periodic boundary condition. Although this rotor simulation approach yields detailed flow field information, it is not practical in terms of problem set up and full helicopter modeling. A second methodology is also used in which rotor simulation is done with a boundary condition based on blade element – momentum method.

The ducted rotor geometry of the Kamov KA-60 tail rotor is selected as the test case and analyses results obtained in this study are compared with previously published experimental and analyses results [5], [10].

PROBLEM DESCRIPTION

The tail rotor of the Kamov Ka-60 helicopter is chosen as the ducted rotor model which was tested at TsAGI[5] and analyzed by Kwon et. al [10]. The geometrical details of the chosen model, such as shroud radial thickness and geometry of the vertical fin, are not available in literature, hence some simplifications on the model are applied. In the simplified model, the vertical fin is neglected and the shroud geometry is simplified to an axially symmetric one. After simplifications, the model becomes very similar to the one analyzed by Kwon et. al. [10]. The specifications of the analyzed baseline model is given below in Table 1.

Table 1 Specifications of the baseline rotor

Rotor	Radius	0.297 m
	Number of blades	11
	Solidity	0.4951
	Twist angle	-12 degrees
	Tip speed	74.6 m/s (Mtip= 0.22)
	Airfoil	NACA 23012 (r/R=0.35~1.0)
Shroud	Tip clearance gap	0.01R
	Inlet radius	0.2R
	Diffuser length	0.7R
	Diffuser angle	4 degrees

The tail rotor model has 11 equally spaced blades which have rectangular tip shapes. Tip clearance between the blades and the shroud equals to one percent of the blade radius.

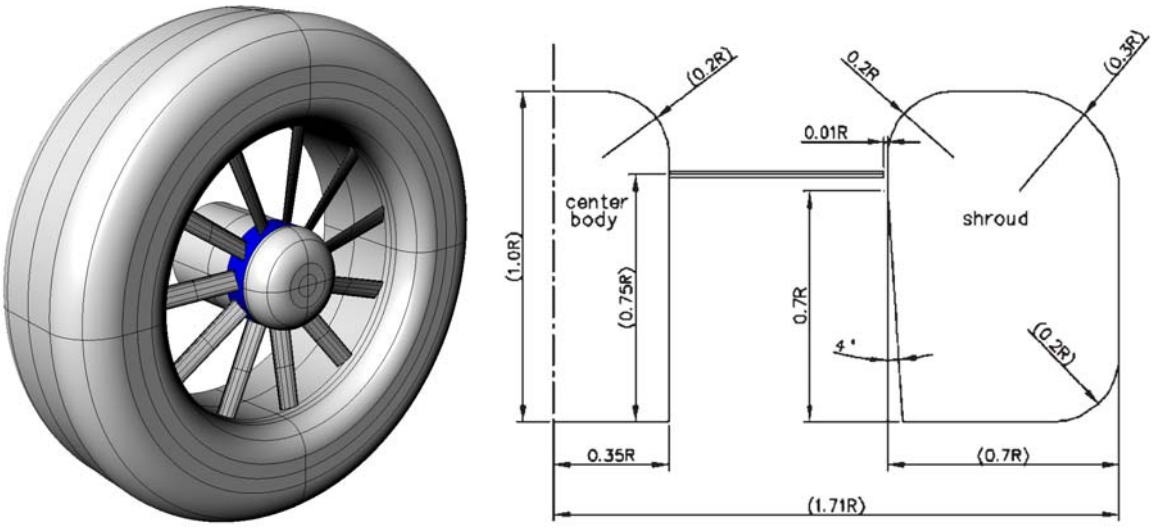

a) Isometric view of the rotor model b) Sketch of the model at axisymmetric plane

Figure 1 Geometry of the test case model

COMPUTATIONAL MODEL AND NUMERICAL SCHEMES

CFD analyses are carried out by using the commercial flow solver FLUENT. Three dimensional, double precision solver is utilized for the solution of the problem. The segregated solution with SIMPLE scheme is performed for the Navier Stokes flow equations. Turbulence properties are evaluated by the k-w SST model. The reference length of the flow is chosen as blade radius and the rotor disc area is used to evaluate non dimensional coefficients.

Two different approaches are used for the solution of the flow at hover conditions. For the first alternative, the unsteady flow solution around the individual blade is carried out by using rotating reference frame and periodic boundary conditions. In the second alternative, the rotor blades excluded from the solution and the time averaged cumulative effects of the rotor disk is modeled by the blade element-momentum method.

Rotating reference frame and periodic boundary condition

The analyzed ducted rotor model has an axisymmetric duct and the blades are spaced equally. Hence, the flow properties between the rotor blades will be periodic in hover conditions. To simplify the numerical analyses, individual flow domain bound by two blades is evaluated rather than analyzing the whole domain around the rotor. Periodic boundary conditions are set for the boundaries of the domain in tangential direction. The analyzed domain is divided into two sub-zones. The inner zone is bounded by periodic faces, hub geometry and shroud wall. The boundaries of the inner zone in axial direction are set at half blade chord distance away from the rotor blade. To represent the rotor motion, rotating reference frame is defined for the inner domain. The outer zone, which is defined by stationary reference frame, extends from inner zone to outer far field boundary. The analyzed flow domain is presented in Figure 2.

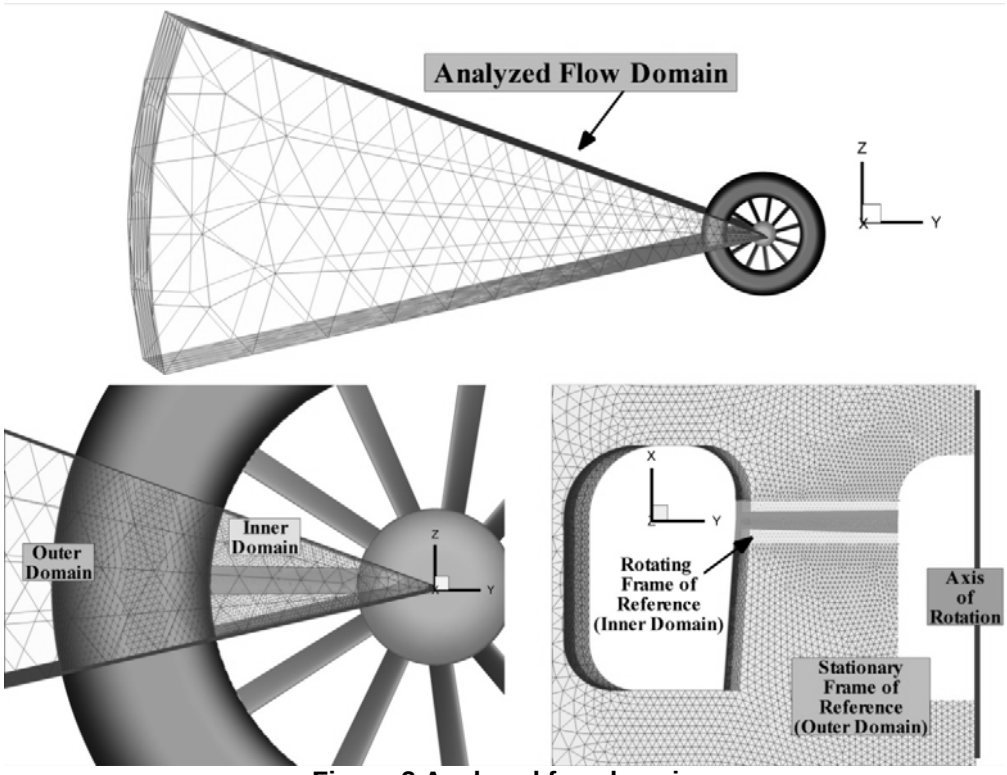

Figure 2 Analyzed fow domain

Non-slip wall boundary conditions are set on the rotor blades and shroud. The pressure far field boundary conditions are defined for the outmost boundaries of the outer zone in axial and radial directions. To mesh the wall boundaries of the inner zone, 78000 triangular elements that are mostly clustered around the edges and tips of the blade geometry are generated. The surface mesh on the outer zone faces are generated by 116000 elements in total. A finer mesh is used in the regions close to the tip clearance gap and duct walls. To be able to capture the inflow and downwash generated by rotor with minimum mesh size, clustering from the outer boundary to the rotation axis is applied.

Volume mesh is generated by utilizing commercial tool Tgrid. 15 layers of prism cells are constructed on the wall surfaces to resolve the boundary layer, causing the use of 865000 elements. The cells in the first layer are located such that y+ values are around 1. The Reynolds number at the half span of the blade is calculated as $1.5x10^5$.

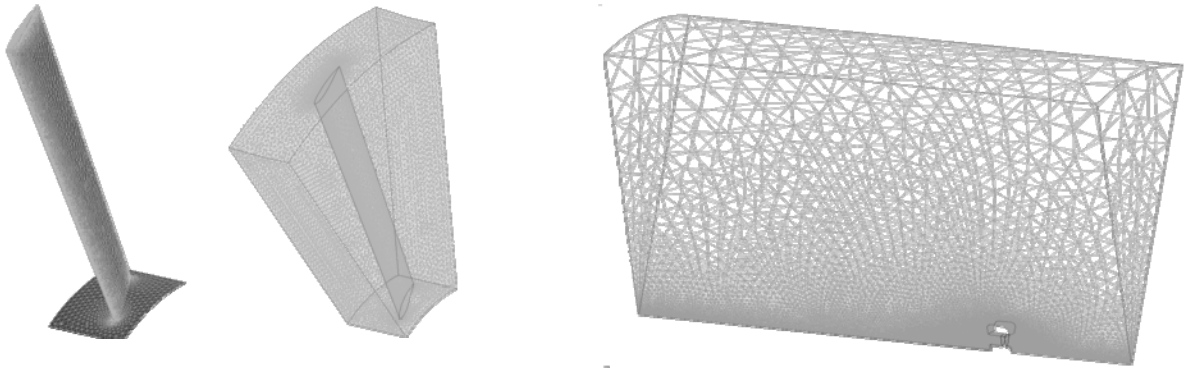

a) Blade only b) Blade and inner domain c) Outer boundary

Figure 3 Surface mesh on the rotor blades and boundaries

Blade element-momentum boundary condition

The solution of the Navier Stokes equations with the rotating blades leads to an expensive solution scheme. Simulating the rotor disk effects rather than directly including the blades in the solution domain is a popular way of decreasing the cost of analysis. The exclusion of the blades reduces the complexity and the size of the mesh significantly. Moreover, by dealing with the time averaged cumulative effects rather than instantaneous properties, it is possible to evaluate critical specifications of the rotors, such as thrust production, with much less effort.

Blade element-momentum model [12] is used as a boundary condition for the alternative solution to the rotating reference frame with periodic boundary condition. In the rotor disk plane, momentum sources that vary in radial and tangential directions are introduced into the NS equations to define a pressure jump through the rotor. To evaluate the magnitude of the momentum sources, the blade element theory is utilized. Utilizing this approach, it is possible to introduce the coning, flapping, collective and cyclic angles of the rotor into the solution cheaply. Along the rotor span, varying design characteristics such as twist, airfoil type and chord length can also be tested.

The disk created by blade tip path is extruded shortly in the axial direction and the momentum source terms are defined in that zone. A small region is left between the cylinder and duct wall to represent tip clearance. Wall surfaces are meshed by unstructured elements and prism cells are constructed on them for viscous solutions. The pressure far field boundary conditions are implemented on the outer boundary surfaces and the flow domain is meshed with tetrahedral cells. The short cylinder is filled with single layer of prism cells. The model and volume mesh used in this approach is presented in Figure 4.

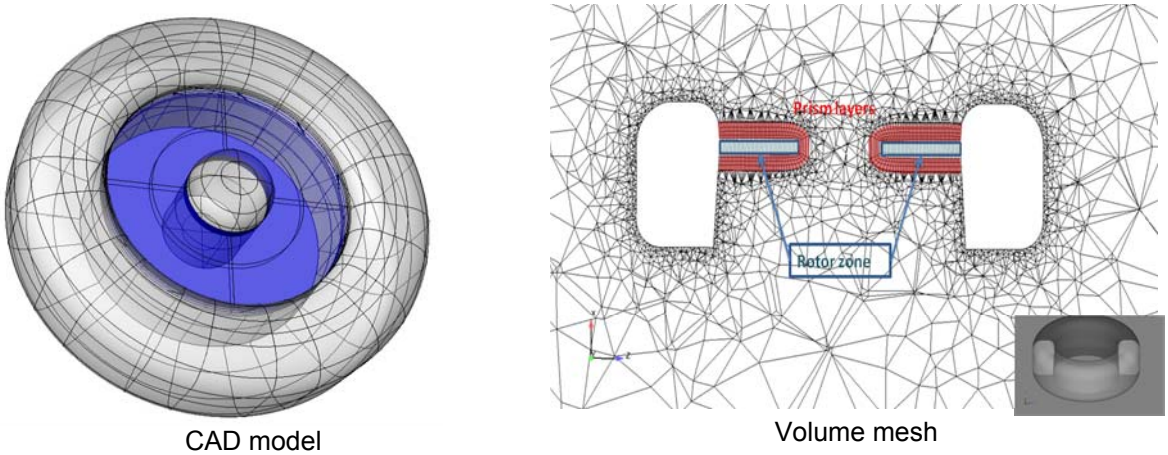

CAD model Volume mesh

Figure 4 Model analyzed by second approach

RESULTS

The results obtained in this study are compared with the results published by Boris et. al[5] and Kwon et.al[10]. Boris et al. presented experimental results on the Ka-60 tail rotor model at 45 degrees collective angle and Lee et al. published numerical results for a simplified rotor model at 40 and 45 degrees of collective angle. The experimental results show that at hover conditions the blades of the Ka-60's shrouded rotor produces 88 N thrust when the blade root collective angle is 45 degrees[5]. The model analyzed in this study is axially symmetric and does not include vertical fin effects. Hence, those simplifications would result in a slight variation of the rotor flow and thrust. Using the rotating reference frame method, flow solutions are evaluated for different collective angles to figure out the case at which simplifications on the geometry are paid off. The variation of the generated thrust force with respect to changing collective angles is drawn in Figure 5. In the figure, both of the total thrust and the force generated by the blades are presented. Using the given plot, it is found that decrement of the collective angle by three degrees from 45 to 42 compensates the geometrical simplifications that affect the flow acceleration through the rotor disc. The comparisons of the results are performed for converged solutions. Figure 6 represents the convergence monitor of the solutions, where the variation with respect to blade revolutions is analyzed. It is shown that at all collective angle settings, approximately after 5 revolutions of the rotor blades, the flow field reaches steady state and ratio of the total thrust to thrust of the blades, which is called augmentation ratio, converges to the theoretical limit, 2.

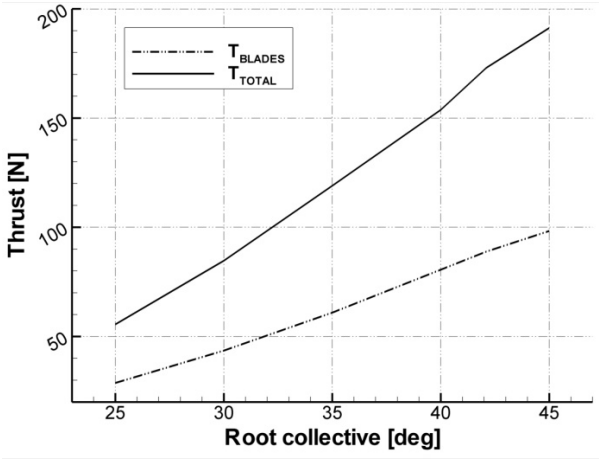

Figure 5 Change of rotor thrust by varying collective angle

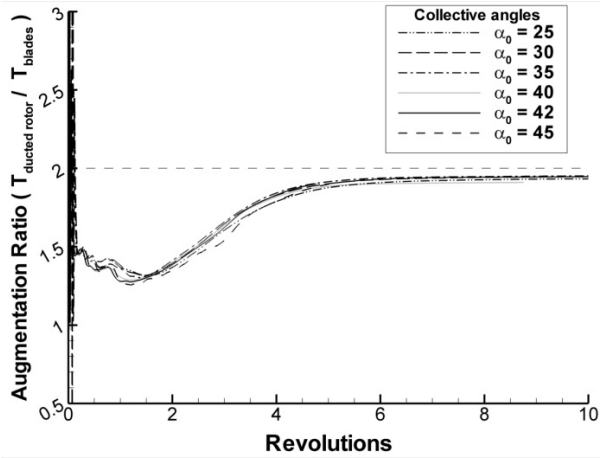

Figure 6 Variation of augmentation ratio by revolutions of rotor

Evaluating the steady solution and extracting the collective angle setting that produces identical thrust force on the blades with experimental results, the resultant sectional loading on the blades are compared with the published results in Figure 7.

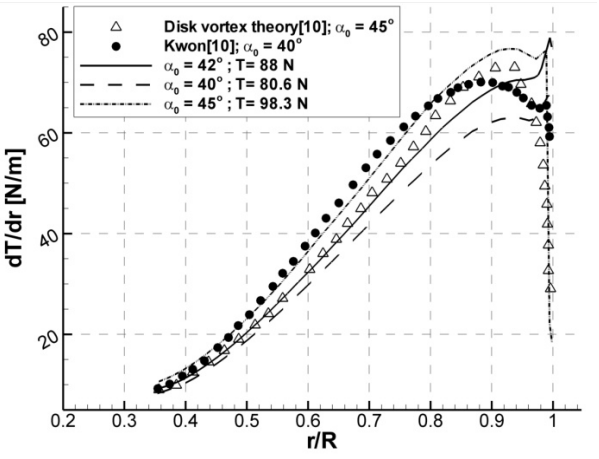

Figure 7 Comparison of sectional thrust loading on blades

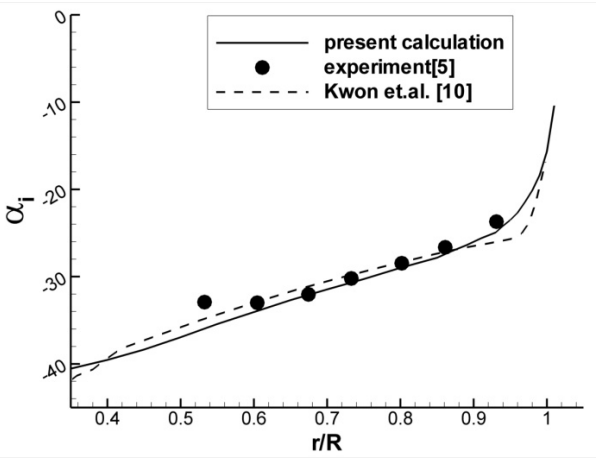

Figure 8 Comparison of induced angle of attack

In figure 7, the numerically generated results of this study is represented by lines and the results published by Kwon et al[10] for the 88 N thrust generation cases are represented by symbols. Compared to “disk vortex theory”[10] all numerical analysis result in less three dimensional flow near the tip region and the loss of load is smaller. Excluding the tip region, the evaluated load distribution in this study is closer to disk vortex theory than the inviscid solutions presented in Reference 10. It is also observed that the results generated for 45 degrees of collective angle setting, which produces higher thrust, compares better with their results. This dissimilarity originates from the difference of the flow equations that are solved, i.e. Euler solutions should be leading to higher loading than the Navier Stokes solution performed in this study.

The calculated induced angle of attack and velocity components are compared with previously published experimental and numerical results for validation purpose in figures 8 and 9. The experimental data is represented by dots, previously published numerical results are represented by dashed lines and the results of the present study are given by lines in the corresponding plots. The comparisons of the flow field data are performed for the plane located half chord distance below the rotor disk. The evaluated flow variables are averaged azimuthally and variation of the mean values in radial direction are judged against published experimental results. The x-axis of the figures represents the radial coordinates normalized by rotor disk radius. The hub geometry extends from origin to 35 percent radius and the duct geometry is located at 101 percent radius. As illustrated in the figures, evaluated numerical results are reliable and consistent with the available data. The calculated induced angle of attack magnitude compares very well with the experiment from hub to tip. Evaluated axial velocity component is in good agreement with the previously published results in sections close to the hub, however both numerical studies evaluated higher axial velocity components compared to the experiment. Nevertheless, the axially induced velocity calculated in the present study, approximately fits to the experimental data from 60 percent radius to tip, although published numerical results have discrepancies close to the tip region. The present study also calculates a closer induced tangential velocity distribution to experimental ones compared to results of Kwon et.al. Similar to the induced axial velocity results, tangential component calculations also deviate from the experiment in regions close to the hub. Moreover, at the tip region, numerical evaluation brings out a tangential velocity increment which is not observed in the experiment.

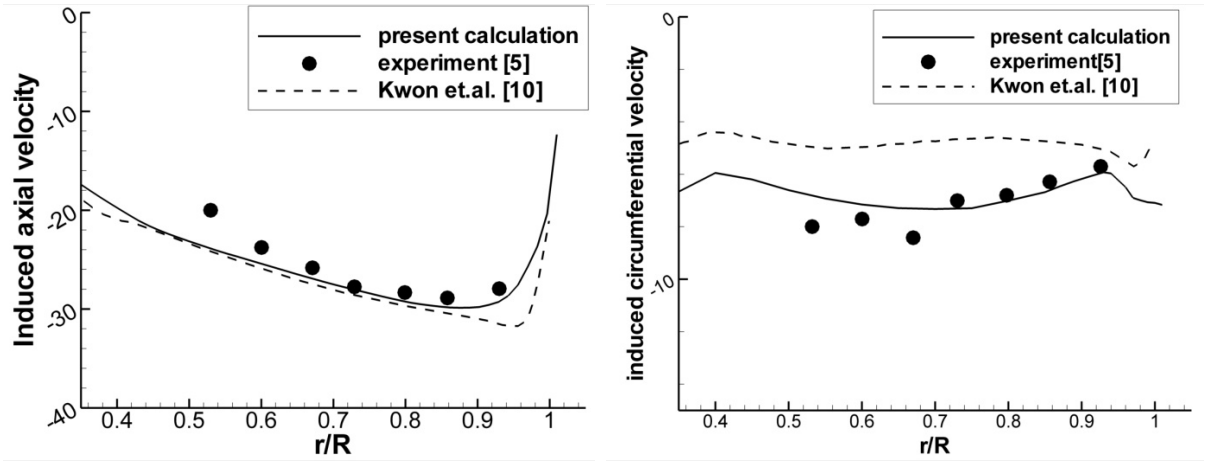

a) Comparison of induced downwash velocity b) Comparison of induced circumferential velocity

Figure 9 Comparison of induced velocities by rotor

Obtaining satisfactory results from the examination of the accuracy of the rotating reference frame method, the potential of blade element momentum (BEM) boundary condition method is analyzed. Two different airfoil tables are used to reflect the change of flow conditions at the root and the tip. In order to account for the tip losses, the rotor disk is assumed to produce no lift but only the drag in the region extending from 99 percent rotor radius to tip. Steady flow solution is performed for the case where the root collective angle equals 42 degrees. The BEM boundary condition method generates consistent results and 88 N of thrust force is evaluated on the rotor disk when the solver is converged. However the augmentation ratio of the ducted rotor is calculated to be slightly smaller than the rotating reference frame method with a value of 1.81.

Figure 10 presents the axial velocity contours through the ducted rotor in hover conditions where collective angle is 42 degrees. The right and left halves of the plot are evaluated by two different methods mentioned earlier. The presented planes are clipped at constant azimuth, which cuts the

blade at the quarter chord line. Examining the magnitude and variation of the axial velocity in the duct it can be commented that both methods evaluate consistent flow solutions. The differences on the contours are due to the dissimilarity in the solution strategies and the meshes used for the two solutions.

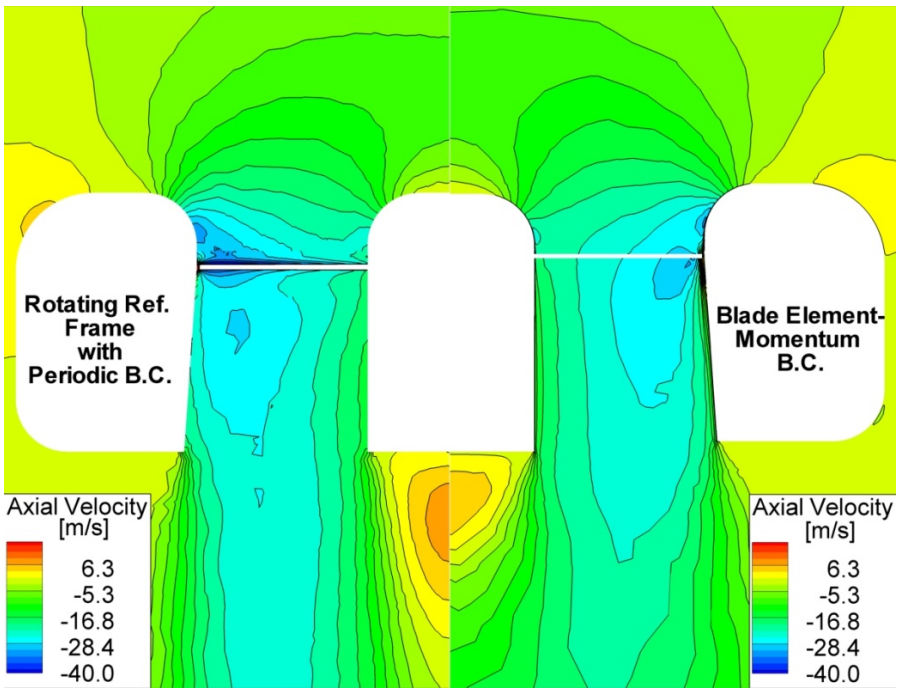

Figure 10 Axial velocity contours at constant azimuth plane

The evaluated axial velocity variation in radial direction is used as another measure for the judgment of the two solution techniques. The flow variables are averaged circumferentially on planes parallel to the tip path plane, located at 0.15R above and 0.5R below of the rotor. The comparison of the radial variation of the averaged axial velocities on those planes is presented in Figure 11. In the figure, the y axes are normalized by 30 m/s, which is approximately the highest axial velocity magnitude read in Figure-9.

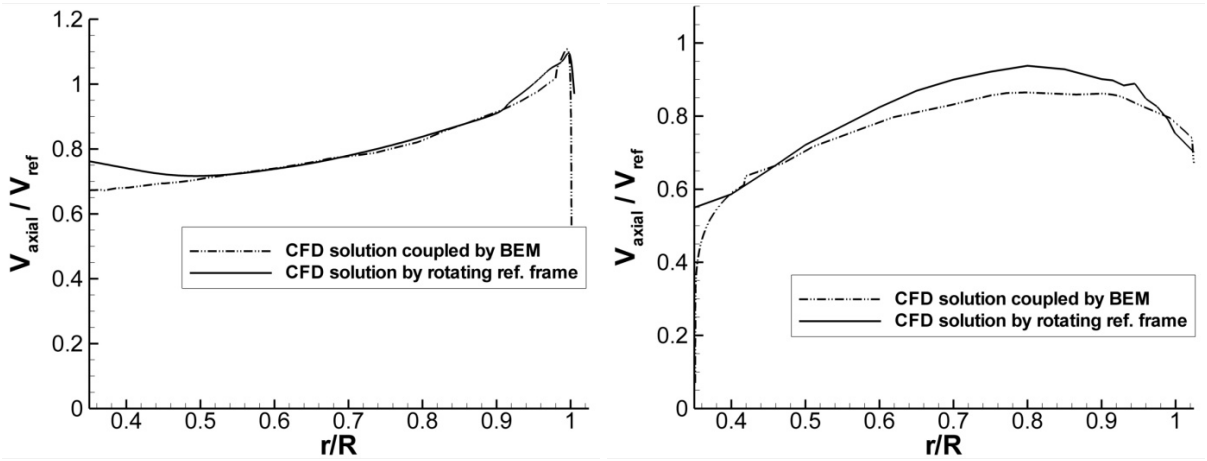

a) 0.15R upstream of the rotor disk b) 0.5R downstream of the rotor disk

Figure 11 Comparison of normalized axial speed distribution

In Figure 11, the evaluated axial velocities by both methods compares well with each other except near walls, at the upstream plane. This discrepancy originates from the difference in the resolution of the meshes used by two techniques. Due to its lower cost, the duct and hub walls are meshed much finer in BEM boundary condition type solution method and the descent of the velocity due to presence of the walls reflects more significantly on the plots. At the downstream plane, while the evaluated variation is reliable for both techniques, rotating reference frame method with periodic boundary conditions is found to generate slightly higher axial velocities. Even though the general characteristics of the rotor system such as thrust and augmentation ratio has evaluated with good consistency, a

further study in mesh refinement and adaptation is required to be able to extract identical flow field properties by both methods.

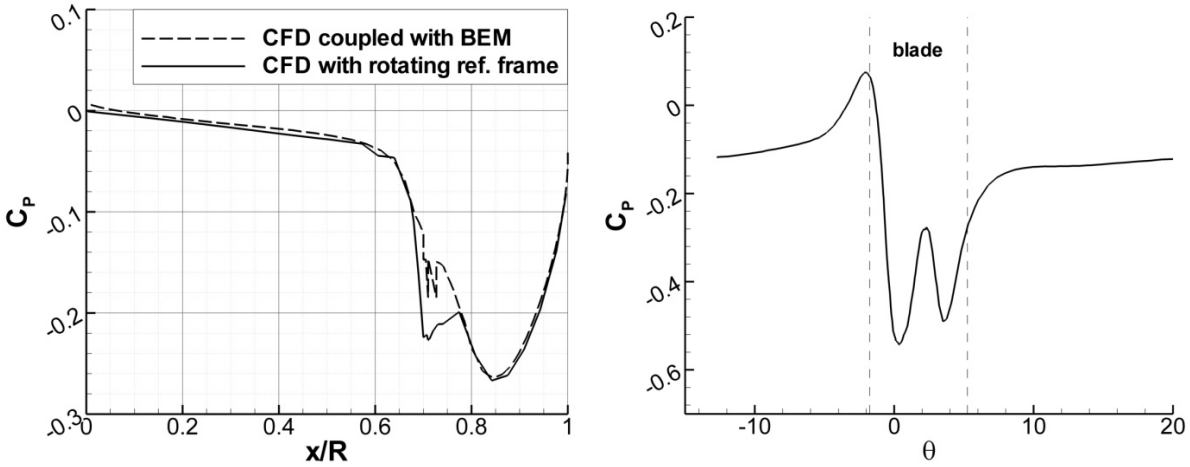

a) Variation of circumferentially averaged pressure on duct wall in axial direction

b) Azimuthally variation of pressure on duct wall just above the rotor tip path plane

Figure 12 Pressure variation along the duct geometry

The variation of the gauge pressure on the inner duct surface from inlet to outlet is presented in Figure 12. In the figures, the y axis represents the gauge static pressure normalized by the dynamic pressure that is evaluated using the rotor tip speed. In Figure 12(a), variations of the circumferentially averaged pressures in axial directions are compared. Both solutions yield almost identical results except the region close to the rotor plane. The negative pressure peaks on the duct lip where a great amount of the thrust of the duct is generated. The method in which motion of the blades is simulated, greater pressure increase on the duct surface is observed near the rotor disk. This is a rational result since high velocity gradients due to tip clearance gap could be captured more precisely by this method compared to its BEM boundary condition type alternative. The origin of the discrepancy seen in pressure variation is presented by Figure 12(b) where the tangential variation of the pressure on the duct, just above the blades is drawn for the rotating reference frame method. The steep gradients due to the forced flow through the pressure side of the blades to suction side causes suction pressure peaks on the duct wall near the tip gap.

CONCLUSION AND DISCUSSION

Aerodynamics of the ducted tail rotor is analyzed numerically. Blade motion is represented by definition of rotating reference frame and required mesh size is decreased by application of periodic boundaries. The methodology followed is validated by the previously published data and satisfactory results are obtained. An alternative way of ducted rotor aerodynamics analysis is examined by simulation of the rotor disk as a boundary condition that is based on blade element-momentum theory. Both methods generate consistent results in evaluation of general characteristics of the rotor system. Agreement on mean flow characteristics through the duct is also captured with reasonable accuracy. The method based on coupling CFD with blade element momentum theory is found to be a good alternative for discrete analysis of blade motion when large numbers of flow solutions are required for the general characteristics of the system. Regarding both methods, CFD is an efficient tool to analyze the ducted rotor flow field and can be used by aerodynamicists to evaluate potential of new designs and to perform design optimizations.

Acknowledgements

The authors present special thanks to Emre Gürdamar for his valuable contributions to the numerical analyses.

REFERENCES

[1] Mouille, R., "The Fenestron, Shrouded Tail Rotor of the SA. 341 Gazelle", *Journal of the American Helicopter Society,* Vol. 15, No. 4, 1970, pp. 31-37.

[2] Clemmons, M. G. "Antitorque safety and the RAH-66 Fantail", Proceedings 48th AHS Annual Forum, Vol. 1, pp. 169-175, 1992

[3] Clark, D.,R., "Aerodynamic design rationale for the fan-in-fin of the S-67 helicopter", Proceedings of 31st AHS Annual National Forum, 1975

[4] Rajagopalan, R. G. and Keys, C. N., "Detailed Aerodynamic Analysis of the RAH-66 FANTAIL

[5] Bourtsev, B. N., and Selemenev, Serguei, V., "Fan-in-fin Performance at Hover Computational Method," 26th European Rotorcraft Forum, The Hague, Netherlands, Sep 26–29, 2000, Paper No. 10.

[6] Alpman, E., and Long, L. N., "Unsteady RAH-66 Comanche Flowfield Simulations Including Fan-in-fin," 16th AIAA Computational Fluid Dynamics Conference, Orlando, FL, Jun 23–26, 2003, no. AIAA-2003-4231

[7] Costes, M., Gavériaux, R. and Renaud T., Application of CFD to the Computation of Complex Rotorcraft Configurations", Proceedings of European Congress on Computational Methods in Applied Sciences and Engineering, ECCOMAS 2004

[8] Ruzicka, G. C., Strawn, R. C., and Meadowcroft, E. T., "Discrete-Blade, Navier-Stokes Computational Fluid Dynamics Analysis of Ducted-Fan Flow," Journal of Aircraft, Vol. 42, No. 5, Sep–Oct 2005, pp. 1109–1117

[9] Nygaard, T. A., Dimanlig, A. C., and Meadowcroft, E. T., "Application of a Momentum Source Model to the RAH-66 Comanche FANTAIL," AHS 4th Decennial Specialists' Conference on Aeromechanics, San Francisco, CA, Jan 21–23, 2004.

[10] Lee, H. D., Kwon, O. J., and Joo, J., "Aerodynamic Performance Analysis of a Helicopter Shrouded Tail Rotor Using an Unstructured Mesh Flow Solver," 5th Asian Computational Fluid Dynamics, Busan, Korea, Oct 27–30, 2003, Paper No. 8.

[11] Cao, Y., Yu, Z. "Numerical simulation of turbulent flow around helicopter ducted tail rotor",Aerospace Science and Technology, Vol. 9,Issue 4, pp. 300-306, 2005

[12] Ruith, M.,R., "Unstructured, Multiplex Rotor Source Model With Thrust And Moment Trimming - Fluent's VBM Model", 23rd AIAA Applied Aerodynamics Conference, AIAA 2005-5217, June 2005, Toronto, Canada